begell house, inc.

Vicky Lipowski
Production Manager
50 Cross Highway
Redding, Connecticut 06896
Phone: 1-203-938-1300
Fax: 1-203-938-1304
Email: vicky@begellhouse.com

Article Reference #: 0401-003
Date Proof Sent: 3-6-07
Total Pages: 17

Journal: International Journal for Multiscale Computational Engineering

Year: 2006 **Volume**: 4 **Issue**: 1

Article Title: Multi-scale Total Lagrangian Formulation for Modeling Dislocation Induced Plastic Deformation in Polycrystalline Materials

Dear Prof. Jiun-Shyan Chen:

Attached is a PDF file containing the author proof of your article. If you are unable to access this file, please let me know and I will fax your proof.

This is your only opportunity to review the editing, typesetting, figure placement, and correctness of text, tables, and figures. Answer copyeditor's queries in the margin. Failure to answer queries will result in the delay of publication of your article, so please make sure they are all adequately addressed. **You will not be charged for any corrections to editorial or typesetting errors; however, you will be billed at the rate of $25 per hour of production time for rewriting, rewording, or otherwise revising the article from the version accepted for publication ("author's alterations"); any such charges will be invoiced and must be paid before the article is published.**

Please return your corrections in one of the following ways: (1) Fax: Clearly mark your corrections on the page proofs and fax the **corrected pages only**, along with the offprint order form, if applicable. (2) E-mail: Indicate your corrections in a list, specifying the location of the respective revisions as precisely as possible. Please **DO NOT** annotate the PDF file.

The deadline for your corrections or your notification that you have reviewed the proof and have no corrections is 48 hours after receipt of your proof. No article will be published without confirmation of the author's review. If we do not hear from you within the allotted time, we will be happy to hold your article for a future issue, to give you more time to make your corrections.

Attached is a form for ordering offprints, issues, or a subscription. As corresponding author, you will receive a complimentary copy of this issue. If you wish to order extra issues or offprints, please fill in the appropriate areas and fax the form to me with your corrections.

Thank you for your assistance, and please reference **JMC0401-003** in your correspondence. Also, kindly confirm receipt of your proofs.

Sincerely,

Vicky

Vicky Lipowski
Production Manager

begell house, inc.

JOURNAL PRODUCTION DEPARTMENT
50 Cross Highway
Redding, Connecticut 06896
203-938-1300 (Phone)
203-938-1304 (Fax)
vicky@begellhouse.com

Journal Name: Int J for Multiscale Computational Engineering

Volume/Issue #: Volume 4, Issue 1

Article Title: JMC0401-003 Multi-scale Total Lagrangian Formulation for Modeling Dislocation Induced Plastic Deformation in Polycrystalline Materials

BILL TO:

SHIP TO:

Dear Prof. Jiun-Shyan Chen:

As corresponding author, you will receive a complimentary copy of this issue. Please use the order form below to order additional material and/or indicate your willingness to pay for color printing of figures (if applicable).

To purchase individual subscriptions or a personal copy of your article, please go to www.begellhouse.com Allow approximately 3 weeks, from receipt of your page proofs, for the issue to be posted to our website. For institutional pricing on PDF files contact Dahlia De Jesus at 1-203-938-1300 or dahlia@begellhouse.com

If placing an order, this form and your method of payment must be returned with your corrected page proofs. Please include cost of shipment as indicated below; checks should be made payable to Begell House, Inc., and mailed to the above address. If a purchase order is required, it may arrive separately to avoid delaying the return of the corrected proofs.

OFFPRINTS OF ARTICLE*

PAGE COUNT OF ARTICLE
(round off to highest multiple of 8)

QTY.	**4**	**8**	**16**	**24**	**32**
25	72	115	151	187	223
50	84	127	163	199	236
100	108	193	254	314	375
200	156	327	435	544	652
300	205	459	616	773	930

***If your page count or quantity amount is not listed please email a request for prices to vicky@begellhouse.com

Black and White Offprints: Prices are quoted above

Offprint Color Pages: Add $3 per color page times the quantity of offprints ordered

Shipping: Add 20% to black and white charge

Offprint Qty: __________ $ ____________

Color Pages for Offprints: $ ____________

Shipping Charges: $ ____________

WIRE TRANSFER

Bank: **Valley National Bank**
Routing #: **0 2600 6 790**
Account #: **07 011343**

CREDIT CARD PAYMENT

CREDIT CARD # ______________________________

NAME ON CREDIT CARD ________________________

AMEX/ VISA/MC/ DISC/ EURO/ _______ EXP. _________

OTHER: __________________________________

CORPORATE PURCHASE ORDER

P. O. # ________________________________

PAYMENT BY CHECK

INCLUDE THE FOLLOWING INFO ON YOUR CHECK:
Article Reference # and Offprints/Color/Subscription

Make checks payable to Begell House, Inc.

COST FOR COLOR PAGES PRINTED IN JOURNAL

Price Per Color Pg.: $ ____________

Number of Color Pages: ____________

Total Cost for Color Pages in Journal: $_______

COPY OF JOURNAL ISSUE (AUTHOR DISCOUNT)

Price Per Copy: **$____** **Number of Copies**:_____

Total Cost for Copies: $: ________

SUBSCRIPTION — 2006

Institutional Subscription$_____* 6 Issues Per Year *Add $10.00 for shipments outside the United States

REVISED 2/11/06

Multiscale Total Lagrangian Formulation for Modeling Dislocation-Induced Plastic Deformation in Polycrystalline Materials

*Xinwei Zhang, Shafigh Mehraeen, Jiun-Shyan Chen**

Civil & Environmental Engineering Department, University of California, Los Angeles (UCLA), 5731G Boelter Hall, Los Angeles, CA 90095, USA

Nasr Ghoniem

Mechanical and Aerospace Engineering, University of California, Los Angeles, Los Angeles, CA 90095, USA

ABSTRACT

Multiscale mathematical and computational formulation for coupling mesoscale dislocation mechanics and macroscale continuum mechanics for prediction of plastic deformation in polycrystalline materials is presented. In this development a total Lagrangian multiscale variational formulation for materials subjected to geometric and material nonlinearities is first introduced. By performing scale decomposition of kinematic variables and the corresponding dislocation kinematic variables, several leading-order equations, including a scale-coupling equation, a mesoscale dislocation evolution equation, and a homogenized macroscale equilibrium equation, are obtained. By further employing the Orowan relation, a mesoscopic plastic strain is obtained from dislocation velocity and its distribution, and a homogenized elastoplastic stress-strain relation for macroscale is constructed. The macroscale, mesoscale, and scale-coupling equations are solved interactively at each macroscopic load increment, and information on the two scales is passed through the macroscale integration points. In this multiscale approach the phenomenological hardening rule and flow rule in the classical plasticity theory are avoided, and they are replaced by a homogenized mesoscale material response characterized by dislocation evolution and their interactions.

KEY WORDS

*Address all correspondence to jschen@seas.ucla.edu

0731-8898/05/$35.00

1. INTRODUCTION

Plastic deformation in metals occurs mainly due to the breaking and reforming of atomic bonds, which allows dislocations to glide through crystalline materials. This process, together with dislocation mutual interactions as well as interactions with other mesoscopic defects, results in a heterogeneous plastic deformation in crystalline grains. The macroscale phenomenological description of material plastic behavior has intrinsic limitations in incorporating mesoscale information and local defects in the material law.

The classical theory of dislocations has led to significant understanding of the behavior of individual crystal defects and elementary interactions among them. However, it does not seem to be well suited to the description of the highly organized and complex behavior of dislocation populations under dynamic conditions. For that reason, two new approaches have emerged over the last decade: direct computer simulation of dislocation dynamics [1–3] of the collective dynamics of dislocations and the self-organization approach [4–6] for describing dislocation structure formation. The computer simulation approach incorporates the behavior of individual dislocations, as known from classical theory, and the complexity of their interactions is explicitly handled by numerical methods. For example, Kubin and Canova [7] and Kubin *et al.* [8] divided dislocation lines into pure edge and screw segments without any mixed dislocations, which requires small segmentation as well as a large number of subsegments during the dislocation evolution. H. M. Zbib and others [9,10] proposed another model based on a straight segment with mixed character. A superdislocation model was also introduced to deal with the long-range dislocation interactions. Ghoniem *et al.* [3] and Ghoniem and Sun [11] developed the parametric dislocation dynamics approach by utilizing parametrized curves to describe the dislocation lines that yield enhanced computational accuracy and efficiency.

The mathematical theory of homogenization has been introduced by Bensoussan *et al.* [12]. Multiscale methods have received significant attention in recent years, and many of these developments have been applied to the modeling of heterogeneous materials [13–17]. The homogenized Dirichlet projection method by Oden *et al.* [18] and Oden and Zohdi [19] was developed based on the concept of hierarchical modeling. In this method the mathematical model at the coarsest level is represented by homogenized material properties. This is referred to as the homogenized problem, and the exclusion of heterogeneity generally makes the homogenized problem computationally inexpensive compared to models of finer scale. An error estimate was developed for identifying the error between the coarse-scale solution using homogenized properties and the fine-scale solution of the heterogeneous material with microstructures [19]. This approach was further extended to a hierarchical modeling of heterogeneous materials where the most essential scales of the problem can be adaptively selected in the discretization [18]. In the asymptotic expansion approach introduced by Bensoussan *et al.* [12] the relationship between the coarse-scale and fine-scale solution can be derived, and the corresponding homogenized differential operator and homogenized coefficients for solving the macroscopic solution can be obtained. This method has been applied to multiscale modeling of microstructural evolution in the process of grain growth by Chen and Mehraeen [13,14]. Alternatively, a multigrid method for a periodic heterogeneous medium has been introduced by Fish and Belsky [20] and Fish and Shek [21]. In this approach a multigrid method was employed to develop a fast iterative solver for differential equations with oscillatory coefficients. An intergrid transfer operator was constructed following the asymptotic expansion so that the problem on the auxiliary grid gives rise to a homogenization problem. Wavelet-based multiscale homogenization has been introduced by Dorobantu and Engquist [22], Chen and Mehraeen [13], and Mehraeen and Chen [23] for problems with fixed microstructures.

For inelastic materials, Fish *et al.* [24] introduced a multiscale analysis of composites, where continuum plasticity in the matrix is taken into consideration. On the basis of the two-scale asymptotic expansion of the displacement field, a close form expression relating eigenstrains in the inclusion to the mechanical fields was derived, and an averaging theorem was employed for solving the overall structural response. This work considered small strain in the macroscopic structure. A multiscale approach presented by Smit *et al.* [25] considered a large deformation effect, in which the micro-macro structural relations in large deformations were obtained, and the method was implemented in a multilevel finite element framework. In the context of nonlinear analysis a homogenization-based multiscale method was also proposed by Cricri and Luciano [26], where a macroscopic failure surface is defined with microstructure taken into consideration. Recently, a homogenization method was proposed by Takano *et al.* [27,28], in which the scale-coupling function between macroscopic and mesoscopic variables was defined in a general, nonlinear form. Although the aforementioned approaches introduced multiscale formulation for modeling inelastic behavior of heterogeneous materials, the phenomenological laws have been employed.

This work aims to develop a multiscale variational and computational formulation, which allows the modeling of plastic deformation in a continuum by incorporating mesoscopic dislocation evolution and the corresponding homogenized stress-strain relation in a multiscale framework. In this approach the averaged plastic strain in the microstructure is obtained by the mesoscopic simulation of dislocation evolution, and this information is utilized to form the homogenized elastoplastic tangent modulus for macroscopic computation. The mesoscopic deformation and dislocation evolution are linked to the macroscopic deformation through the integration points in the macroscopic continuum. The outline of this paper is as follows. Section 2 reviews dislocation mechanics and describes how plastic strain and elastoplastic tangent modulus can be constructed in grain structures. In Section 3, the variational equation for coupled continuum mechanics and dislocation mechanics is presented, and scale decomposition based on asymptotic expansion is introduced. The multiscale variational equations, including a scale-coupling equation, the mesoscale dislocation evolution equation, and a homogenized macroscale equilibrium equation, are derived. The linearization of these multiscale equations for general nonlinear problems as well as numerical procedures for multiscale computation are also presented in this section. Numerical procedures of the proposed multiscale formulation are given in Section 4. In Section 5, a numerical example demonstrating multiscale modeling of the elastoplastic behavior of a CS.016 cold-worked carbon steel is presented. Conclusion remarks are outlined in Section 6.

2. OVERVIEW OF DISLOCATION MECHANICS

Plastic deformation in polycrystalline materials can be described microscopically by considering point defects (vacancies interstitials and impurities), dislocations, grain boundaries, microcracks, and voids in grain structures. In this work, discrete dislocation evolution is modeled to characterize the plastic yielding and hardening process. The internal length scales within grain structure, such as Burgers vector and dislocation density, are embedded in the mesoscopic model. In what follows, dislocation mechanics is introduced as the basic mechanism of plastic deformation via a multiscale homogenization.

2.1 Discrete Description of Dislocation Mechanics

The primary mechanisms at the mesoscale level controlling plastic deformation in continuum are the dislocation formation, evolution, and interactions between dislocation loops [3,10,16,22]. In this work, two-dimensional geometry and the double slip systems with discrete edge dislocations are considered in each grain as shown in Fig. 1. Frank-Read sources, shown as solid dots in Fig. 1(b), are introduced at discrete nucleation points. Periodic boundary conditions are imposed for both dislocation motions and grain boundary geometry.

Following Ghoniem *et al.* [3], the virtual work of a dislocation motion can be expressed as

$$\delta E_d^I = \oint_{S_d^I} \delta \mathbf{r} \cdot \mathbf{f}_{PK} ds - \oint_{S_d^I} \delta \mathbf{r} \cdot \mathbf{B} \cdot \hat{\mathbf{v}} ds \qquad (2.1)$$

where $\mathbf{B}$ is the inverse mobility matrix, $\hat{\mathbf{v}}$ is the dislocation velocity, S_d^I is the Ith dislocation loop, and $\mathbf{f}_{PK}$ is the Peach-Koehler force, which is defined as

$$\mathbf{f}_{PK} = [(\boldsymbol{\sigma} + \boldsymbol{\sigma}^d) \cdot \mathbf{b}] \times \boldsymbol{\xi}, \qquad (2.2)$$

where $\boldsymbol{\sigma}$ is the external applied Cauchy stress field, $\boldsymbol{\sigma}^d$ is the Cauchy stress field induced by other dislocations, $\mathbf{b}$ is the Burger's vector, and $\boldsymbol{\xi}$ is the dislocation line vector as shown in Fig. 2. In two dimensions the equation of motion (Eq. (2.1)) can be simplified in the following linear drag relationship:

$$\hat{\mathbf{v}} = M_g \mathbf{f}_{PK} \qquad (2.3)$$

where M_g is the mobility of dislocation glide. Here we assume that the motion of dislocation is limited to glide along the slip plane, and the dislocation climbing process related to high temperature is not considered.

Following the general coordinate convection for two interacting dislocations as shown in Fig. 2, the stress tensor $\boldsymbol{\sigma}^d$ of an arbitrary test dislocation is given by

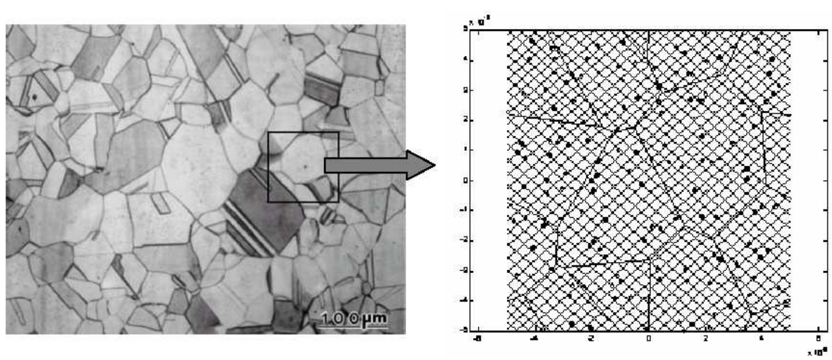

(a) (b)

FIGURE 1. **(a)** Microstructure of AL-6XN stainless steel; **(b)** unit cell/microstructure with grain boundaries and slip planes utilized in multiscale analysis

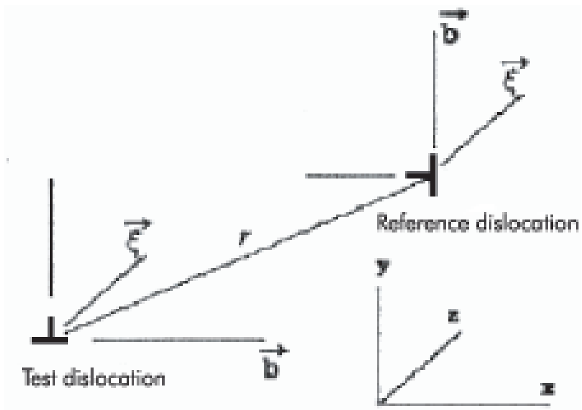

FIGURE 2. General coordinate convection for two interacting dislocations

$$\sigma^d = \frac{\mu b}{2\pi(1-\upsilon)} \begin{bmatrix} -\frac{r_x(3r_x^2+r_y^2)}{(r_x^2+r_y^2)^2} & \frac{r_x(r_x^2-r_y^2)}{(r_x^2+r_y^2)^2} & 0 \\ \frac{r_x(r_x^2-r_y^2)}{(r_x^2+r_y^2)^2} & \frac{r_y(r_x^2-r_y^2)}{(r_x^2+r_y^2)^2} & 0 \\ 0 & 0 & -\frac{2r_y}{r_x^2+r_y^2} \end{bmatrix} \quad (2.4)$$

where r_x and r_y are the components of position vector measured in the coordinate system shown in Fig. 2, b is the magnitude of Burgers vector, μ is shear modulus, and υ is Poisson's ratio.

Dislocation multiplication is introduced by Frank-Read source points, which generate new dislocations when the resolved shear stress is beyond the critical nucleation stress over a given nucleation time period. Annihilation of two dislocations on the same slip plane with opposite Burgers vectors occurs when they are within critical annihilation distance. In addition, if the resolved shear stress on a dislocation is below the friction stress, the dislocation becomes immobilized. It can be remobilized if the resolved shear stress is higher than the friction stress. The plastic deformation of a crystalline material is largely dependent on the ability for dislocation to move within a material. Therefore grain structural parameters that impede the movement of dislocations, such as the existence of grain boundaries, results in reducing plastic deformation of the material. In this work we consider grain boundaries as the energy barrier of dislocation motions, and transmission and absorption of dislocations across grain boundaries are ignored.

2.2 Dislocation and Plastic Deformation

On the basis of Orowan [29], the plastic strain rate produced by gliding dislocations can be expressed as

$$\dot{\boldsymbol{\epsilon}}^p = \rho_m \bar{v} b \mathbf{M} \quad (2.5)$$

where ρ_m is the mobile dislocation density, $\bar{v}$ is the average dislocation velocity, b is magnitude of Burgers vector, and $\mathbf{M}$ is the Schmid tensor of slip system, defined as

$$\mathbf{M} = \tfrac{1}{2}(\mathbf{m} \otimes \mathbf{n} + \mathbf{n} \otimes \mathbf{m}) \quad (2.6)$$

where $\mathbf{m}$ is slip direction and $\mathbf{n}$ is slip plane normal direction. On the basis of the discrete dislocation mechanics and Orowan equation, the plastic strain rate in a double slip system, as shown in Fig. 1(b), can be expressed as

$$\dot{\boldsymbol{\epsilon}}^p = \tfrac{1}{2}\sum_i \rho_m^{(i)} \bar{v}^{(i)} b (\mathbf{m}^{(i)} \otimes \mathbf{n}^{(i)} + \mathbf{n}^{(i)} \otimes \mathbf{m}^{(i)}) \quad (2.7)$$

where i is a given slip system. Further considering strain rate $\dot{\boldsymbol{\epsilon}}$, decomposition into elastic strain rate $\dot{\boldsymbol{\epsilon}}^e$ and plastic strain rate $\dot{\boldsymbol{\epsilon}}^p$:

$$\dot{\boldsymbol{\epsilon}} = \dot{\boldsymbol{\epsilon}}^e + \dot{\boldsymbol{\epsilon}}^p \quad (2.8)$$

A general stress-strain rate relation can be expressed by

$$\dot{\boldsymbol{\sigma}} = \mathbf{C} : \dot{\boldsymbol{\epsilon}}^e \quad (2.9)$$

where $\dot{\boldsymbol{\epsilon}}$ is the Cauchy stress rate and $\mathbf{C}$ is the elastic modulus tensor. Substituting Eqs. (2.7) and (2.8) into Eq. (2.9), we have

$$\dot{\boldsymbol{\sigma}} = \mathbf{C} : \left[\dot{\boldsymbol{\epsilon}} - \tfrac{1}{2}\rho_m \bar{\mathbf{v}} b (\mathbf{m} \otimes \mathbf{n} + \mathbf{n} \otimes \mathbf{m})\right] \tag{2.10}$$

3. COUPLED DISLOCATION AND CONTINUUM MECHANICS

3.1 Variational Equation

Define macroscopic and mesoscopic coordinates as shown in Fig. 3 in the undeformed configuration as $\mathbf{X}$ and $\mathbf{Y}$, respectively, and macroscopic and mesoscopic coordinates in the deformed configuration as $\mathbf{x}$ and $\mathbf{y}$, respectively. To start, we consider a continuum with a domain Ω_X and boundary $\Gamma_X = \Gamma_X^h \cup \Gamma_X^g$, subjected to an external traction $\mathbf{h}$ and body force $\mathbf{b}$. At any point $\mathbf{X}$ in the macroscale domain, there is an associated representative mesoscale unit cell describing the fine-scale material heterogeneity and deformation expressed in both mesoscale coordinate $\mathbf{Y}$ and macroscale coordinate $\mathbf{X}$. To set up the multiscale variational equation, we first account for all the macro- and mesoscale features and mechanisms in the continuum domain Ω_X. If a virtual material displacement $\delta\mathbf{u}$ and a virtual dislocation motion $\delta\mathbf{r}$ are imposed on this system, we have the following variational equation:

$$\begin{aligned} &\int_{\Omega_X} \delta u_{i,J} P_{ji} d\Omega \\ &+ \sum_{I=1}^{NUC\times ND} \left(\oint_{S_d^I} \delta r_i \mathbf{f}_{PK_i} ds - \oint_{S_d^I} \delta r_i B_{ij} \hat{\mathbf{v}}_j ds \right) \\ &- \int_{\Omega_X} \delta u_i b_i d\Omega - \int_{\Gamma_X^h} \delta u_i h_i d\Gamma = 0 \end{aligned} \tag{3.1}$$

with boundary conditions

$$\begin{aligned} P_{ji} N_j &= h_i \quad on \quad \Gamma_X^h \\ u_i &= g_i \quad on \quad \Gamma_X^g \end{aligned} \tag{3.2}$$

where Γ_X^h and Γ_X^g are natural and essential boundaries in the undeformed configuration, respectively, $(.)_{,J} = \partial(.)/\partial X_j$, P_{ji} is first Piola-Kirchhoff stress, b_i is the body force defined in Ω_X, h_i is the surface force divided by the undeformed surface area, N_j is the surface normal defined on Γ_X^h, $\mathbf{B}$ is the inverse mobility matrix, $\hat{\mathbf{v}}$ is the dislocation velocity, $\mathbf{f}_{PK}$ is the

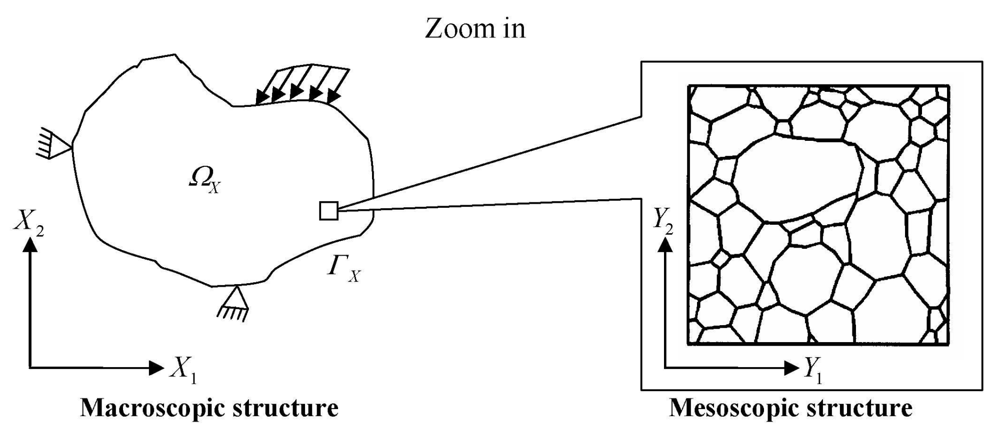

FIGURE 3. Micro- and mesocoordinate systems

Peach-Koehler force, S_d^I is the Ith dislocation loop, NUC is the total number of mesoscale unit cells in Ω_X, and ND is the total number of dislocations within each mesoscale unit cell. It is understood immediately that since this equation is expressed in the macroscale domain with all macroscale and mesoscale features considered, incorporating all dislocation loops on this scale is computationally impossible. In Section 3.2, a multiscale decomposition of macroscale and mesoscale kinematic variables will be introduced so that certain variables are only solved at their appropriate scale level, and a scale-coupling relation will be introduced to bridge variables at different scales.

3.2 Multiscale Decomposition

Define a representative mesoscale unit cell in the mesoscale coordinate with domain Ω_Y as shown in Fig. 4, and periodicity in the unit cell at any deformation state is assumed. The interrelation of macroscopic and mesoscopic coordinates in the undeformed configuration is identified by

$$Y_i = \frac{X_i}{\lambda} \tag{3.3}$$

where the scale ratio λ is a very small number. Similarly, Eq. (3.3) in deformed configuration reads

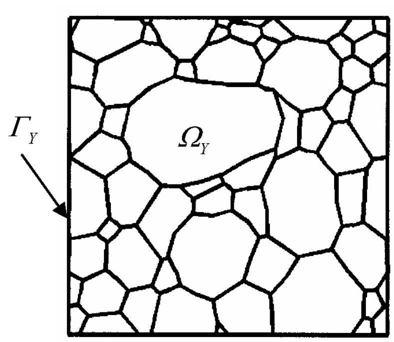

FIGURE 4. Periodic grain structure with domain Ω_Y and Γ_Y boundary

$$y_i = \frac{x_i}{\lambda} \tag{3.4}$$

For notational convenience in this work, any multiscale variable t is defined in the following asymptotic form

$$t = t^{[0]} + \lambda t^{[1]} + O\left(\lambda^2\right) \tag{3.5}$$

where t is the mesoscopic variable, $t^{[0]}$ is referred to as the macroscopic variable (coarse-scale component of t), and $t^{[1]}$ is defined as the fine-scale component of t.

By employing the asymptotic theory, the mesoscopic displacement in the unit cell (with fixed $\mathbf{X}$) measured using mesoscopic coordinates can be expressed by the asymptotic expansion in Eq. (3.5) (scaled by $1/\lambda$) to yield

$$u_i\left(\mathbf{Y}\right) = \frac{1}{\lambda} u_i{}^{[0]}\left(\mathbf{X}\right) + u_i{}^{[1]}\left(\mathbf{X,Y}\right) \qquad \text{(holding } \mathbf{X} \text{ fixed)} \tag{3.6}$$

where $u_i\left(\mathbf{Y}\right)$ is the mesoscopic displacement and $u_i{}^{[0]}\left(\mathbf{X}\right)$ and $u_i{}^{[1]}\left(\mathbf{X,Y}\right)$ are coarse- and fine-scale components of displacement, respectively. Here, the coarse-scale component $u_i{}^{[0]}\left(\mathbf{X}\right)$ is independent of mesoscale coordinate $\mathbf{Y}$, whereas $u_i{}^{[1]}\left(\mathbf{X,Y}\right)$ is a perturbed term caused by the heterogeneity of the grain structure.

Furthermore, we adopt the following coarse-fine scale interrelation

$$u_i{}^{[1]}(\mathbf{X,Y}) = \alpha_{kli}(\mathbf{Y})\left(\frac{\partial u_k{}^{[0]}}{\partial X_l}\right) = \alpha_{kli}(\mathbf{Y}) F_{kl}^{[0]} \tag{3.7}$$

where the coupling function $\alpha_{kli}\left(\mathbf{Y}\right)$ is independent of macroscopic coordinates $\mathbf{X}$. From the stress-strain relation, and considering that the coarse-scale component of displacement is independent of mesoscopic coordinates $\mathbf{Y}$, Cauchy stress can be expressed as

$$\boldsymbol{\sigma}_{ij} = \boldsymbol{\sigma}_{ij}^{[0]} + \lambda \boldsymbol{\sigma}_{ij}^{[1]} + O\left(\lambda^2\right) \tag{3.8}$$

Consequently, the dislocation velocity $\hat{\mathbf{v}}$ and dislocation stress $\boldsymbol{\sigma}^d$ induced by the multiscale stress field can be expressed by the same asymptotic form:

$$\hat{\mathbf{v}} = \hat{\mathbf{v}}^{[0]} + \lambda \hat{\mathbf{v}}^{[1]} + O\left(\lambda^2\right) \tag{3.9}$$

$$\boldsymbol{\sigma}^d = \boldsymbol{\sigma}^{d[0]} + \lambda \boldsymbol{\sigma}^{d[1]} + O\left(\lambda^2\right) \tag{3.10}$$

where $\hat{\mathbf{v}}^{[0]}$ and $\hat{\mathbf{v}}^{[1]}$ are the dislocation velocities induced by the coarse-scale and fine-scale stress fields, respectively, and $\boldsymbol{\sigma}^{d[0]}$ and $\boldsymbol{\sigma}^{d[1]}$ are the corresponding coarse- and fine-scale dislocation-induced stresses, respectively. Introducing Eq. (3.8) into Eq. (2.2) gives rise to

$$\begin{aligned}\mathbf{f}_{PK}(\boldsymbol{\sigma}, \boldsymbol{\sigma}^d) = {} & \mathbf{f}_{PK}^{[0]}(\boldsymbol{\sigma}^{[0]}, \boldsymbol{\sigma}^{d[0]}) \\ & + \lambda \mathbf{f}_{PK}^{[1]}(\boldsymbol{\sigma}^{[1]}, \boldsymbol{\sigma}^{d[1]}) + O\left(\lambda^2\right)\end{aligned} \tag{3.11}$$

$$\boldsymbol{\sigma}_{PK}^{[0]}(\boldsymbol{\sigma}^{[0]}, \boldsymbol{\sigma}^{d[0]}) = [(\boldsymbol{\sigma}^{[0]} + \boldsymbol{\sigma}^{d[0]}) \cdot \mathbf{b}] \times \boldsymbol{\xi}, \tag{3.12}$$

$$\mathbf{f}_{PK}^{[1]}(\boldsymbol{\sigma}^{[1]}, \boldsymbol{\sigma}^{d[1]}) = [(\boldsymbol{\sigma}^{[1]} + \boldsymbol{\sigma}^{d[1]}) \cdot \mathbf{b}] \times \boldsymbol{\xi}, \tag{3.13}$$

Subsequently, the energy due to an evolving dislocation follows the same asymptotic form:

$$\begin{aligned}\delta E_d^I &= \oint_{S_d^I} \delta \mathbf{r} \cdot \mathbf{f}_{PK} ds - \oint_{S_d^I} \delta \mathbf{r} \cdot \mathbf{B} \cdot \hat{\mathbf{v}} ds \\ &= \oint_{S_d^I} \delta r \cdot \mathbf{f}_{PK}^{[0]} ds - \oint_{S_d^I} \delta \mathbf{r} \cdot \mathbf{B} \cdot \hat{\mathbf{v}}^{[0]} ds \\ &\quad + \lambda \left(\oint_{S_d^I} \delta \mathbf{r} \cdot \mathbf{f}_{PK}^{[1]} ds - \oint_{S_d^I} \delta \mathbf{r} \cdot \mathbf{B} \cdot \hat{\mathbf{v}}^{[1]} ds \right) + O\left(\lambda^2\right) \\ &= \delta E_d^{I[0]} + \lambda \delta E_d^{I[1]} + O\left(\lambda^2\right)\end{aligned} \tag{3.14}$$

where

$$\delta E_d^{I[0]} = \oint_{S_d^I} \delta \mathbf{r} \cdot \mathbf{f}_{PK}^{[0]} ds - \oint_{S_d^I} \delta \mathbf{r} \cdot \mathbf{B} \cdot \hat{\mathbf{v}}^{[0]} ds \tag{3.15}$$

$$\delta E_d^{I[1]} = \oint_{S_d^I} \delta \mathbf{r} \cdot \mathbf{f}_{PK}^{[1]} ds - \oint_{S_d^I} \delta \mathbf{r} \cdot \mathbf{B} \cdot \hat{\mathbf{v}}^{[1]} ds \tag{3.16}$$

To obtain multiscale variational equations, Eqs. (3.6) and (3.14) are introduced to the variational Eq. (3.1) to yield

$$\begin{aligned}&\int_{\Omega_X} \left(\frac{\partial \delta u_i^{[0]}}{\partial X_j} + \frac{\partial \delta u_i^{[1]}}{\partial Y_j} \right) P_{ji} d\Omega \\ &+ \sum_{I}^{NUC \times ND} (\delta E_d^{I[0]} + \lambda \delta E_d^{I[1]}) \\ &= \int_{\Omega_X} \left(\delta u_i^{[0]} + \lambda \delta u_i^{[1]} \right) b_i d\Omega \\ &+ \int_{\Gamma_X^h} \left(\delta u_i^{[0]} + \lambda \delta u_i^{[1]} \right) h_i d\Gamma\end{aligned} \tag{3.17}$$

in which we used the scaling relation in Eq. (3.3) and employed the following chain rule:

$$\frac{\partial\,(.)}{\partial X_i} = \frac{\partial\,(.)}{\partial Y_l} \frac{\partial Y_l}{\partial X_i} = \frac{1}{\lambda} \frac{\partial\,(.)}{\partial Y_i} \tag{3.18}$$

Treating $\delta u_i^{[0]}$, $\delta u_i^{[1]}$, and $\delta \mathbf{r}_i$ as independent variations and considering the limit of $\lambda \to 0$, Eq. (3.17) gives rise to three multiscale variational equations:

3.2.1 Scale-Coupling Equation

$$\int_{\Omega_X} \frac{\partial \delta u_i^{[1]}}{\partial Y_j} P_{ji}(\boldsymbol{\sigma}^d, \hat{\mathbf{v}}, u) d\Omega = 0 \tag{3.19}$$

where the fine-scale variable $u_i^{[1]}$ is related to the coarse-scale variable $\frac{\partial u_k^{[0]}}{\partial X_l}$ via the scale-coupling function $\alpha_{kli}\left(\mathbf{Y}\right)$, as given in Eq. (3.7).

Note that the first Piola-Kirchhoff stress is a function of dislocation evolution. This equation is to be used to solve for the coupling function $\alpha_{kli}(\mathbf{Y})$, where the details will be discussed in the next section.

3.2.2 Macroscale Equilibrium Equation

$$\int_{\Omega_X} \frac{\partial \delta u_i^{[0]}}{\partial X_j} P_{ji}(\boldsymbol{\sigma}^d, \hat{\mathbf{v}}, u) d\Omega = \int_{\Omega_X} \delta u_i^{[0]} b_i d\Omega + \int_{\Gamma_X^h} \delta u_i^{[0]} h_i d\Omega \tag{3.20}$$

where the homogenized stress-strain relationship required in this macroscale equation is to be obtained from the scale-coupling function solved in Eq. (3.19) and the mesoscale dislocation evolution equation given below.

3.2.3 Mesoscale Dislocation Evolution Equation

Utilizing the coarse-scale component of the strain obtained by Eq. (3.20), the third decoupled equation gives rise to

$$\sum_{I=1}^{NUC \times ND} \delta E_d^{I[i]} = 0, i = 0, 1 \tag{3.21}$$

from which dislocation velocity $\hat{\mathbf{v}}^{[i]}$ can be solved. Separating the summation operator in Eq. (3.21) into two levels, one over each unit cell, and the other over all unit cells in the domain Ω_X reads

$$\sum_{m=1}^{NUC} \sum_{l=1}^{ND} \left(\oint_{S_d^{l,m}} \delta\mathbf{r} \cdot \mathbf{f}_{PK}^{[i]}(\boldsymbol{\sigma}^{[i]}, \boldsymbol{\sigma}^{d[i]}) ds - \oint_{S_d^{l,m}} \delta\mathbf{r} \cdot \mathbf{B} \cdot \hat{\mathbf{v}}^{[i]} ds \right) = 0, \ i = 0, 1 \tag{3.22}$$

where NUC is the total number of unit cells in Ω_X and ND is the total number of dislocations within each unit cell. A sufficient condition to satisfy Eq. (3.22) reads

$$\sum_{l=1}^{ND} \left(\oint_{S_d^l} \delta\mathbf{r} \cdot \mathbf{f}_{PK}^{[i]}(\boldsymbol{\sigma}^{[i]}, \boldsymbol{\sigma}^{d[i]}) ds - \oint_{S_d^l} \delta\mathbf{r} \cdot \mathbf{B} \cdot \hat{\mathbf{v}}^{[i]} ds \right) = 0, \quad i = 0, 1 \tag{3.23}$$

Given coarse-scale components of the strain at quadrature points of global structure, Cauchy stress is computed through an elastic trial predictor at each unit cell. If elastic trial stress is greater than the nucleation stress, Eq. (3.23) is then solved for dislocation velocity $\hat{\mathbf{v}}$, which leads to the incremental plastic strain. Consequently, an elastic trial stress is corrected by means of calculated plastic strain. It is important to note that since the driving force of dislocation evolution is a linear function of stresses $\boldsymbol{\sigma}$ and $\boldsymbol{\sigma}^d$, we have $\mathbf{f}_{PK}^{[0]} + \lambda \mathbf{f}_{PK}^{[1]} = [(\boldsymbol{\sigma}^{[0]} + \lambda \boldsymbol{\sigma}^{[0]}) + (\boldsymbol{\sigma}^{d[0]} + \lambda \boldsymbol{\sigma}^{d[0]}) \cdot \mathbf{b}] \times \boldsymbol{\xi}, = \mathbf{f}_{PK}$. Thus it is straightforward to show that the dislocation velocity can be solved from the combined equation $\sum_{l=1}^{ND} \delta E_d^{l[0]} + \lambda \delta E_d^{l[1]} = \sum_{l=1}^{ND} \delta E_d^l = 0$, i.e.,

$$\sum_{l=1}^{ND} \left(\oint_{S_d^l} \delta\mathbf{r} \cdot \mathbf{f}_{PK}(\boldsymbol{\sigma}, \boldsymbol{\sigma}^d) ds - \oint_{S_d^l} \delta\mathbf{r} \cdot \mathbf{B} \cdot \hat{\mathbf{v}} ds \right) = 0 \tag{3.24}$$

This implies that dislocation velocity can be treated strictly as a mesoscale variable. Although the dislocation evolution equation now can be expressed at the mesoscale level, the stress fields involved in the evolution equation need to be calculated from coarse- and fine-scale displacements that are to be solved from the macroscale equilibrium equation and scale-coupling equations, respectively.

3.3 Linearization of Multiscale Equations

The multiscale Eqs. (3.19) and (3.20) are, in general, nonlinear with respect to u_i, and linearization of these two equations is needed. We first consider that coarse-scale component $u_i^{[0]}(\mathbf{X})$ varies linearly with respect to $\mathbf{X}$ in the mesoscale unit cell:

$$u_i^{[0]}(\mathbf{X}) \approx \left(\partial u_i^{[0]} \big/ \partial X_j\right) X_j = \lambda \left(\partial u_i^{[0]} \big/ \partial X_j\right) Y_j \quad (3.25)$$

in which $u_i(\mathbf{X,Y})$ is measured in macroscopic scale, and we ignore higher-order terms $O(\lambda^2)$. Substituting Eq. (3.25) into the incremental form of Eq. (3.6) yields

$$\Delta u_i(\mathbf{Y}) = \Delta F_{ij}^{[0]} Y_j + \Delta u_i^{[1]}(\mathbf{X,Y}) \quad (3.26)$$

where $\Delta F_{ij}^{[0]} = \partial \Delta u_i^{[0]} \big/ \partial X_j$ is the incremental macroscopic deformation gradient, and incremental fine-scale component of displacement $\Delta u_i^{[1]}(\mathbf{X,Y})$ is obtained from Eq. (3.7) as

$$\Delta u_i^{[1]}(\mathbf{X,Y}) = \alpha_{kli}(\mathbf{Y}) \Delta F_{kl}^{[0]} \quad (3.27)$$

3.3.1 Incremental Scale-Coupling Equation

Introducing Eqs. (3.26) and (3.27) into the incremental form of Eq. (3.19) yields

$$\int_{\Omega_X} \frac{\partial \delta u_i^{[1]}}{\partial Y_j} (D_{ijkl} + T_{ijkl}) \left(\frac{\partial \Delta u_k^{[0]}}{\partial X_l} + \frac{\partial \Delta u_k^{[1]}}{\partial Y_l} \right) d\Omega = -\int_{\Omega_X} \frac{\partial \delta u_i^{[1]}}{\partial Y_j} P_{ji} d\Omega \quad (3.28)$$

where

$$D_{ijkl} = F_{im} C^2_{jmln} F_{kn}, \quad T_{ijkl} = S_{jl} \delta_{ik} \quad (3.29)$$

Here C^2_{jlmn} is the second elasticity tensor and S_{ij} is the second Piola-Kirchhoff stress. Further, substituting Eq. (3.27) into Eq. (3.28) and taking the average over the unit cell gives rise to

$$\int_{\Omega_X} \frac{1}{A_Y} \left[\int_{\Omega_Y} \frac{\partial \delta u_i^{[1]}}{\partial Y_j} (D_{ijkl} + T_{ijkl}) \times \left(\delta_{km} \delta_{nl} + \frac{\partial \alpha_m n k(\mathbf{Y})}{\partial Y_l} \right) d\Omega \right] \frac{\partial \delta u_m^{[0]} \partial X_n}{d} \Omega = -\int_{\Omega_X} \frac{1}{A_Y} \left[\int_{\Omega_Y} \left(\frac{\partial \delta u_i^{[1]}}{\partial Y_j} \right) P_{ji} d\Omega \right] d\Omega \quad (3.30)$$

where A_Y is the area of the unit cell in the undeformed configuration and Ω_Y is the domain of the unit cell. Since the length scale of the mesoscale unit cell is considerably smaller than the macroscopic length scale, the residual (R.H.S.) in the mesoscopic Eq. (3.30) can be ignored, and it yields

$$\int_{\Omega_Y} \frac{\partial \delta u_i^{[1]}}{\partial Y_j} (D_{ijkl} + T_{ijkl}) \frac{\partial \alpha_{mnk}(\mathbf{Y})}{\partial Y_l} dY = -\int_{\Omega_Y} \frac{\partial \delta u_i^{[1]}}{\partial Y_j} (D_{ijmn} + T_{ijmn}) dY \quad (3.31)$$

Note that mesoscale displacement u_i must be used to calculate D_{ijkl} and T_{ijkl} in Eq. (3.31). Once the scale-coupling function α_{mnk} is obtained from Eq. (3.31), the fine-scale incremental displacement can be calculated using Eq. (3.27).

3.3.2 Incremental Macroscale Equilibrium Equation

Substituting Eqs. (3.26) and (3.27) into the incremental equation of Eq. (3.20) and performing an average process over the unit cell, the following incremental equilibrium equation is obtained:

$$\int_{\Omega_X}\frac{\partial\delta u_i{}^{[0]}}{\partial X_j}\left\{\frac{1}{A_Y}\int_{\Omega_Y}(D_{ijkl}+T_{ijkl})\times\left(\delta_{km}\delta_{nl}+\frac{\partial\alpha_{mnk}(\mathbf{Y})}{\partial Y_l}\right)dY\right\}\frac{\partial\Delta u_m{}^{[0]}}{\partial X_n}d\Omega = \int_{\Omega_X}\delta u_i{}^{[0]}b_i d\Omega+\int_{\Gamma_X^h}\delta u_i{}^{[0]}h_i d\Gamma - \int_{\Omega_X}\left(\frac{\partial\delta u_i{}^{[0]}}{\partial X_j}\right)P_{ji}^{[0]}d\Omega \quad (3.32)$$

Recall that the inner integral in Eq. (3.32) is calculated over the unit cell, which leads to homogenized geometric and material response tensors in each unit cell. Recasting the inner integral in Eq. (3.32) leads to homogenized material and geometric response tensors as follows:

$$\bar{D}_{ijmn}=\frac{1}{A_Y}\int_{\Omega_Y}D_{ijkl}\times\left(\delta_{km}\delta_{nl}+\frac{\partial\alpha_{mnk}(\mathbf{Y})}{\partial Y_l}\right)d\Omega \quad (3.33)$$

$$\bar{T}_{ijmn}=\frac{1}{A_Y}\int_{\Omega_Y}T_{ijkl}\times\left(\delta_{km}\delta_{nl}+\frac{\partial\alpha_{mnk}(\mathbf{Y})}{\partial Y_l}\right)d\Omega \quad (3.34)$$

where $\bar{D}_{ijmn}$ is the homogenized material response tensor and $\bar{T}_{ijmn}$ is the homogenized geometric response tensor. Equation (3.32) is rewritten as

$$\int_{\Omega_X}\frac{\partial\delta u_i^{[0]}}{\partial X_j}A_{ijmn}^{[0]}\frac{\partial\Delta u_m{}^{[0]}}{\partial X_n}d\Omega=\int_{\Omega_X}\delta u_i{}^{[0]}b_i d\Omega + \int_{\Gamma_X^h}\delta u_i^{[0]}h_i d\Gamma - \int_{\Omega_X}\left(\frac{\partial\delta u_i{}^{[0]}}{\partial X_j}\right)P_{ji}^{[0]}d\Omega \quad (3.35)$$

$$A_{ijmn}^{[0]}=\bar{D}_{ijmn}+\bar{T}_{ijmn} \quad (3.36)$$

At each macroscopic iteration, homogenized tensor $A_{ijmn}^{[0]}$ is calculated from the unit cell that corresponds to each integration point of the macroscopic structure using the macroscopic information $F_{ij}^{[0]}$. Obtaining the homogenized material property at integration points requires solving the scale-coupling function in Eq. (3.31). With the homogenized material property, the macroscopic displacement increment is computed using Eq. (3.35), and the macroscopic deformation of structure is updated.

It can be easily identified that both the homogenized material response tensor $\bar{D}_{ijmn}$ and the homogenized geometric response tensor $\bar{T}_{ijmn}$ do not possess major symmetry. The symmetry property in the material and homogenized geometric response tensors can be recovered by adopting a consistent homogenization procedure [30], as discussed in Appendix A, where the macroscopic strain energy density $W^{[0]}$ is first calculated, and the homogenized incremental stress-strain relation is then obtained consistently.

The dislocation evolution Eq. (3.23) is a linear function of $\hat{\mathbf{v}}$, and thus the linearized equation takes the same form as the total form equation. The multiscale Eqs. (3.24), (3.31), and (3.35) are solved interactively to yield the complete macroscopic and mesoscopic solutions.

4. NUMERICAL PROCEDURES

In this multiscale analysis the macroscale equilibrium equation is discretized by a coarse mesh for computational efficiency. At each integration point of the macroscopic mesh, the scale-coupling function is solved on the unit cell using the scale-coupling equation and macroscopic stress and strain information. The mesoscopic deformation and stress are then obtained using the scale-coupling function, and this information is employed to calculate dislocation motion using the mesoscopic dislocation evolution equation. The computed dislocation velocities and their distributions are used to obtain plastic deformation of the unit cell. Finally, the homogenized elastoplastic stress-strain relation is returned to the macroscopic equilibrium equation for solving macroscopic deformation at the next load step. These computational procedures are illustrated in Fig. 5.

5. NUMERICAL EXAMPLE

The elastoplastic behavior of a CS.016 cold-worked carbon (0.2% C) steel rod subjected to uniaxial tension is analyzed by the proposed multiscale method, and the results are compared with experimental data reported by Brooks [17]. This model problem is shown in Fig. 6, in which the rod is subjected to an uniaxial tension of 400 MPa. The mesoscopic para-

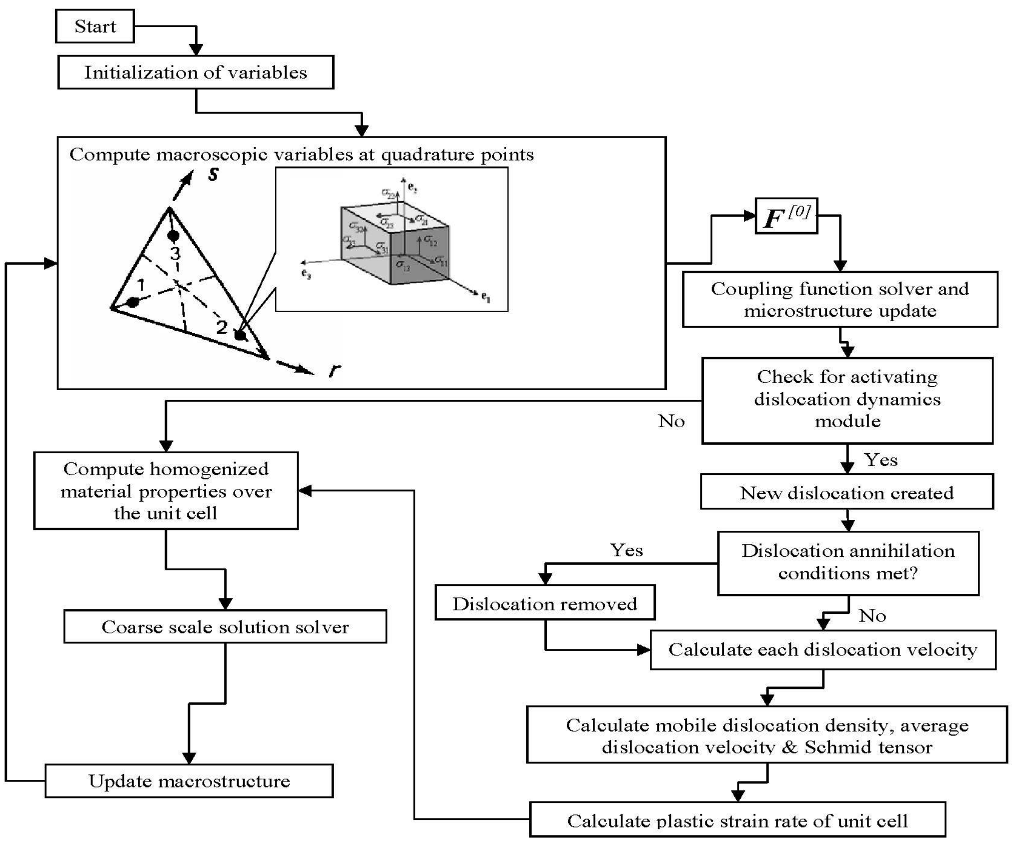

FIGURE 5. Computational algorithm of multiscale analysis

FIGURE 6. CS.016 cold-worked carbon steel rod subjected to an uniaxial tension

meters are given in Table 1. The grain structures of the unit cell (size $= 100\ \mu m \times 100\ \mu m$) are taken from Mehraeen and Chen [23], as shown Fig. 3, and the Young's modulus of each grain is assigned randomly in the range of $E_0 \pm (20\%) E_0$ such that the averaged modulus is consistent with the macroscopic Young's modulus E_0 give in Table 1.

The macroscopic tension increment of $20\ MPa$ is used. At each macroscopic load step, macroscopic strains and stresses based on elastic trial at the integration points are computed. For a given macroscopic incremental strain, mesoscopic incremental displacement is obtained through the scale-coupling function by Eq. (3.31), and consequently, the mesoscopic strain increment is computed. The dislocation computations in the grains are invoked if the trial stress is greater than the dislocation nucleation stress. On the basis of the dislocation calculations given in Section 4, the mesoscopic plastic strain increment is computed, and the elastoplastic tangent operator is returned to the macroscopic integration points for macroscopic equilibrium calculation. Figure 7 shows the evolution of dislocations with increasing strain in the grain structure. The dislocation pileups increase with increasing deformation. The predicted axial stress-strain response, as shown in Fig. 8, agrees well with experimental observations [17].

6. CONCLUSIONS

This work aims to develop a dislocation-based, multiscale formulation for modeling dislocation formation and evolution in grain structures and for characterizing how mesoscale dislocations are related to plastic deformation in the continuum. This paper addresses the following issues: (i) multiscale variational equations between continuum scale and mesoscale for general, large deformation conditions; (ii) coupling of mesoscale dislocations and continuum plastic deformation; (iii) numerical procedures for multiscale modeling of plastic deformation; and (iv) dislocation-based, multiscale analysis of plastic deformation of a CS.016 cold-worked carbon steel without using phenomenological plasticity flow and hardening rules.

An asymptotic, expansion-based, homogenization method incorporated with mesoscale dislocation mechanics has been proposed to provide a systematic approach for multiscale modeling of plastic deformation in polycrystalline materials. To yield the multiscale variational equations and scale-coupling relation, a total Lagrangian formation and its linearization have been adopted. By introducing the asymptotic expansion of the material displacement in the test and trial functions in the variational equation and by averaging strain energy density of the unit cell, the resulting leading-order equations yield the scale-coupling relation, coarse-scale homogenized equilibrium equation, and fine-scale dislocation evolution equation. At every integration point in the macroscopic structure, the pointwise macroscale strain is passed onto the corresponding mesoscale unit cell. Within the mesoscale unit cell, the scale-coupling function was first solved numerically, and mesoscale incremental displacement, strain, and trial stress were computed using the scale-coupling function and macroscale strain information. The mesoscale dislocation evolution in the grain structures was then simulated, and the mesoscale incremental plastic strain was obtained from the dislocation velocity and distribution. By incorporating the scale-coupling function and the mesoscale plastic strain, a homogenized elastoplastic stress-strain relation was obtained and returned to the macroscale integration points. Using the elastoplastic tangent moduli at integration points in the continuum domain, the macroscopic discrete equilibrium equation was constructed and solved. In

TABLE 1. Material properties of AL-6XN stainless-steel and microstructure parameters

Young's modules (E_0)	207 GPa
Poisson's ratio	0.30
Dislocation mobility	$1.1 \times 10^3 \left(Pa^{-1}s^{-1}\right)$
Dislocation nucleation time	3.0×10^{-7}s
Dislocation nucleation stress	150 MPa

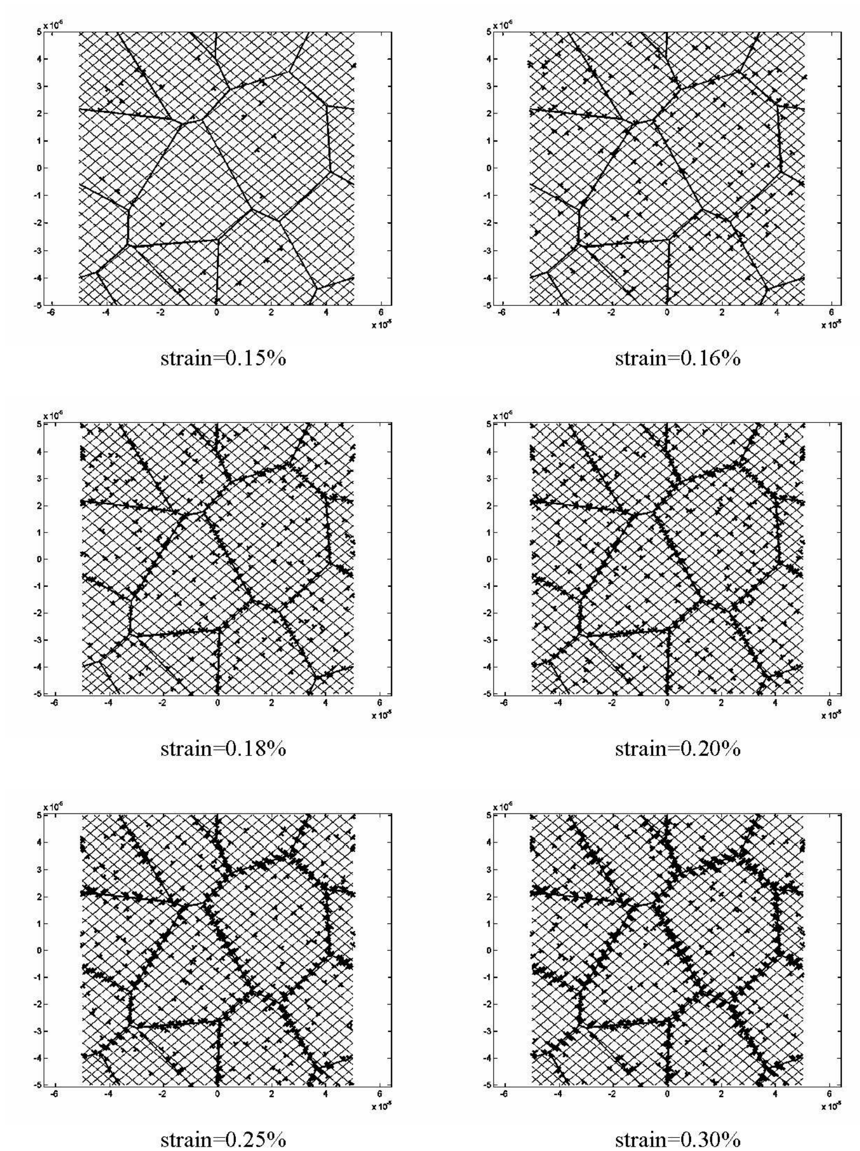

strain=0.15% strain=0.16%

strain=0.18% strain=0.20%

strain=0.25% strain=0.30%

FIGURE 7. Evolution of dislocations at different stain stages

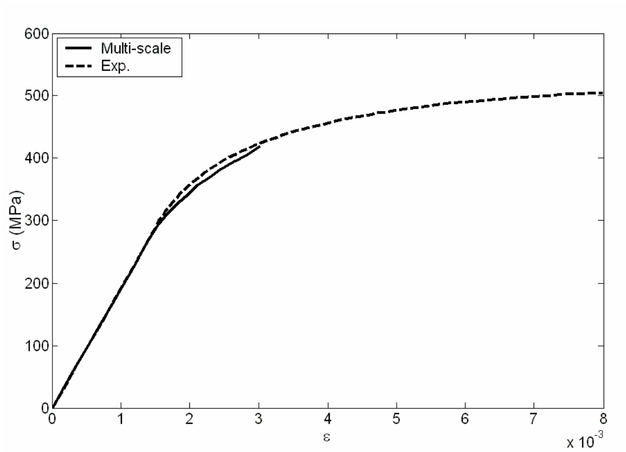

FIGURE 8. Comparison of macroscopic stress-strain curve obtained from proposed multiscale approach with the experimental results of Brooks [17]

this multiscale approach, the phenomenological hardening rule and the flow rule in classical plasticity theory are avoided, and they are replaced by a homogenized mesoscale material response characterized by dislocation evolution and their interactions.

In the numerical example, the elastoplastic deformation of a CS.016 cold-worked carbon steel has been demonstrated. The macroscopic stress-strain response has been obtained by means of the proposed multiscale formulation and numerical algorithms. This stress-strain relation depicted a good agreement with the experimental data.

REFERENCES

1. Devincre, B., and Kubin, L., Three dimensional simulations of plasticity, *Strength of Materials*, Oikawa et al. (Eds.), pp. 179–189, Japan Institute of Metals, 1994.
2. Fournet, R., and Salazar, J. M., Formation of dislocation patterns: Computer simulation, *Phys. Rev.* **53**:6283–6290, 1996.
3. Ghoniem, N. M., Tong, S.-H., and Sun, L. Z., Parametric dislocation dynamics: A thermodynamics-based approach to investigations of mesoscopic plastic deformation, *Phys. Rev. B* **61**:913–927, 2000.
4. Gregor, V., and Kratochvl, J., Self-organization approach to cyclic microplasticity; a model of a persistent slip band, *Int. J. Plasticity* **14**:159–172, 1998.
5. Malygin, G. A., Self organization of dislocations and localization of strain in plastically deformed crystals, *Solid State Phys*. **37**:3–42, 1995.
6. Zaiser, M., Avlonitis, M., and Aifantis, E. C., Stochastic and deterministic aspects of strain localization during cyclic plastic deformation. *Acta Mater*. **46**:4143–4151, 1998.
7. Kubin, L. P., and Canova, G., The modeling of dislocation patterns, *Scr. Metall*. **27**:957–962, 1992.
8. Kubin, L. P., Canova, G., Condat, M., Devincre, B., Pontikis, V., and Brechet, Y., Dislocation microstructures and plastic flow a 3D simulation, *Solid State Phenomena* **23/24**:455–472, 1992.
9. Rhee, M., Zbib, H. M., and Hirth J. P., Models for long/short range interactions in 3D dislocation simulation. *Model. Simul. Mater. Sci. Eng.* **6**:467–492, 1998.
10. Zbib, H. M., Rhee, M., and Hirth, J. P., On plastic deformation and the dynamics of 3D dislocations, *Int. J. Mech. Sci.* **40**:113–127, 1998.
11. Ghoniem, N. M., and Sun, L. Z., Fast sum method for the elastic field of 3-D dislocation ensembles, *Phys. Rev. B* **60**:128–140, 1999.
12. Bensoussan, A., Lions, J. L., and Papanicolau, G., *Asymptotic Analysis for Periodic Structures*, North Holland, Amsterdam, 1978.
13. Chen, J. S., and Mehraeen, S., Multi-scale modeling of heterogeneous materials with fixed and evolving microstructures, *Model. Simul. Mater. Sci. Eng*. **13**:95–121, 2005.
14. Chen, J. S., and Mehraeen, S., Variationally consistent multi-scale modeling and homogenization of stressed grain growth, *Comput. Methods Appl. Mech. Eng*. **193**:1825–1848, 2004.
15. Chen, J. S., Kotta, V., Lu, H., Wang, D., Moldovan, D., and Wolf, D., A variational formulation and a double-grid method for meso-scale modeling of stressed grain growth

in polycrystalline materials, *Comput. Methods Appl. Mech. Eng*. **193**:1277–1303, 2004.

16. Amodeo, R. J., and Ghoniem, N. M., Dislocation dynamics I: a proposed methodology for deformation micromechanics, *Phys. Rev.* **41**:6958–6967, 1990.
17. Brooks, C. R., *Heat Treatment, Structure, and Properties of Nonferrous Alloys*, American Society for Metals, 1982.
18. Oden, J. T., Vemaganti, K., and Moes, N., Hierarchical modeling of heterogeneous solids, *Comput. Methods Appl. Mech. Eng*. **172**:3–25, 1999.
19. Oden, J. T., and Zohdi, T. I., Analysis and adaptive modeling of highly heterogeneous elastic structures, **148**:367–391, 1997.
20. Fish, J., and Belsky, V., Multigrid method for periodic heterogeneous media, 1—Convergence studies for one-dimensional media, *Comput. Methods Appl. Mech. Eng*. **126**:1–16, 1995.
21. Fish, J., and Shek, K., Multi-scale analysis of composite materials and structures, *Compos. Sci. Technol*. **60**:2547–2556, 2000.
22. Dorobantu, M., and Engquist, B., Wavelet-based numerical homogenization, *J. Numer. Anal*. **35**:540–559, 1998.
23. Mehraeen, S., and Chen, J. S., Wavelet-based multi-scale projection method in homogenization of heterogeneous media, finalist of Melosh Medal Competition, *FE Anal. Des.* **40**:1665–1679, 2004.
24. Fish, J., Shek, K., Pandheeradi, M., and Shepherd, M. S., Computational plasticity for composite structures based on mathematical homogenization: theory and practice, *Comput. Methods Appl. Mech. Eng*. **148**:53–73, 1997.
25. Smit, R. J. M., Brekelmans, W. A. M., and Meijer, H. E. H., Prediction of the mechanical behavior of nonlinear heterogeneous systems by multi-level finite element modeling, *Comput. Methods Appl. Mech. Eng*. **155**:181–192, 1998.
26. Cricri, G., and Luciano, R., Micro- and macro-failure models of heterogeneous media with micro-structure, *Simul. Model. Practice Theory* **11**:433–448, 2003.
27. Takano, N., Ohnishi, Y., Zako, M., and Nishiyabu, K., Microstructure-based deep-drawing simulation of knitted fabric reinforced thermoplastics by homogenization theory, *Int. J. Solids Sruct*. **38**:6333–6356, 2001.
28. Takano, N., Ohnishi, Y., Zako, M., and Nishiyabu, K., The formulation of homogenization method applied to large deformation problem for composite materials. *Int. J. Solids Struct*. **37**:6517–6535, 2000.
29. Orowan, E., *Proc. Phys. Soc. London* **52**(8):–, 1940.
30. Chen, J. S., and Mehraeen, S. A., Coupled meso-macro scale formulation for modeling of microstructure evolution and wrinkling formation in polycrystalline materials, *Comput. Methods Appl. Mech. Eng.* (submitted).
31. Nemmat-Nasser, S., Wei, G., and Kihl, D. P., Thermomechanical response of AL-6XN stainless steel over a wide range of strain rates and temperatures, *J. Mech. Phys. Solids* **49**:1823–1846, 2001.
32. Fang, X. C., and Dahl, W., Investigation of the formation of dislocation cell structures and the strain hardening of metals by computer simulation, *Mater. Sci. Eng. A* **164**:300–305, 1993.

APPENDIX A: CONSISTENT HOMOGENIZATION OF THE MACROSCALE EQUILIBRIUM EQUATION

In this section we follow the consistent homogenization method proposed by Bensoussan *et al.* [12]. First, the macroscale strain energy density function is defined by

$$W^{[0]} = \frac{1}{A_Y} \int_{\Omega_Y} W\left(\mathbf{F}\right) d\Omega \tag{A1}$$

$$F_{ij} = \partial u_i / \partial X_j \tag{A2}$$

where **f** and W are the mesoscopic deformation gradient and strain energy density in the unit cell, respectively, and $W^{[0]}$ is the pointwise macroscopic strain energy density. Consequently, it is demonstrated that [12] the macroscopic first PK stress tensor is obtained by

$$P_{ij}^{[0]} = \frac{\partial W^{[0]}}{\partial F_{ji}^{[0]}} = \frac{1}{A_Y}\int_Y \frac{\partial W}{\partial F_{ji}^{[0]}} d\Omega$$
$$= \frac{1}{A_Y}\int_Y P_{nm}K_{nmij} d\Omega \qquad \text{(A3)}$$

$$P_{nm} = \frac{\partial W}{\partial F_{mn}} \qquad \text{(A4)}$$

where

$$K_{nmij} = delta_{jm}\delta_{in} + \eta_{jimn},$$
$$\eta_{klin} = \frac{\partial \alpha_{kli}(\mathbf{Y})}{\partial Y_n} \qquad \text{(A5)}$$

Recasting Eq. (A3) in the incremental form yields

$$\Delta P_{ij}^{[0]} = A_{ijkl}^{[0]} \Delta F_{lk}^{[0]} \qquad \text{(A6)}$$

$$A_{ijkl}^{[0]} = \tfrac{1}{A_Y}\int_{\Omega_Y} A_{pqrs}K_{pqij}K_{rskl} dY,$$

$$A_{pqrs} = \frac{\partial^2 W}{\partial F_{qp}\partial F_{sr}} = C_{pntr}^2 F_{qn}F_{st} + S_{pr}\delta_{sq} \qquad \text{(A7)}$$

Recall that Eq. (A6) demonstrates the major symmetry property of the homogenized first elasticity tensor $A_{ijkl}^{[0]}$. Furthermore, unlike other asymptotic, expansion-based methods [12, 20, 24, 25, 28], the second elasticity tensor in above proposed method also possesses a major symmetry property [12]. On the basis of the incremental form of macroscopic equilibrium Eq. (3.35) and the above consistent homogenization procedures, the macroscopic incremental equation is obtained:

$$\int_{\Omega_X} \frac{\partial du_i^{[0]}}{\partial X_j} A_{ijmn}^{[0]} \frac{\partial \Delta u_m^{[0]}}{\partial X_n} d\Omega = \int_{\Omega_X} du_i^{[0]} b_i d\Omega$$
$$+ \int_{\Gamma_X^h} du_i^{[0]} h_i d\Gamma - \int_{\Omega_X} \frac{\partial du_i^{[0]}}{\partial Y_j} P_{ij}^{[0]} d\Omega \qquad \text{(A8)}$$